Article

Development and Characterization of Pentaerythritol-EudragitRS100 Co-processed Excipients as Solid Dispersion Carriers for Enhanced Aqueous Solubility, *In Vitro* Dissolution, and *Ex Vivo* Permeation of Atorvastatin

Darshan R. Telange,* Neha M. Bhaktani, Atul T. Hemke, Anil M. Pethe, Surendra S. Agrawal, Nilesh R. Rarokar, and Shirish P. Jain

Read Online

ACCESS		Metrics & More		Article Recommendations

ABSTRACT: Atorvastatin (ATV), a lipid-lowering agent, has low oral bioavailability due to its poor water solubility, permeability, and low dissolution rate. Therefore, pentaerythritol-EudragitRS100 co-processed excipients (PECE) were synthesized, and their feasibility as solid dispersion carriers (ATV-PECE-SD) for improving the solubility, permeability, and dissolution rate of ATV was explored. Solid dispersions were assessed in terms of particle size and zeta potential, and solubility, *in vitro* dissolution, and *ex vivo* permeation studies were studied. Scanning electron microscopy (SEM), Fourier transform infrared spectroscopy (FT-IR), differential scanning calorimetry (DSC), and powder X-ray diffraction (PXRD) were used as characterization tools. ATV-PECE-SD3 (1:4) formulations exhibited a small particle size with high stability. Physicochemical evaluation evidenced the formation of solid dispersion due to the involvement of weak electrostatic interaction between the polar functional groups of ATV and PECE carriers. ATV-PECE-SD3 (1:4) significantly enhanced the water solubility by ∼43-fold compared to pure ATV. *In vitro* dissolution studies showed that optimized formulation enhanced the dissolution rate of ATV compared to pure ATV. *Ex vivo* permeation results revealed that ATV-PECE-SD3 (1:4) enhanced the permeation rate of ATV compared to pure ATV. The optimized formulations significantly improved the dissolution rate of ATV in the fed state due to the food effect and micelle formation mechanism compared to the fasted state. The study concludes that co-processed excipients could be used as promising solid dispersion carriers to enhance the aqueous solubility, permeability, and dissolution rate of ATV.
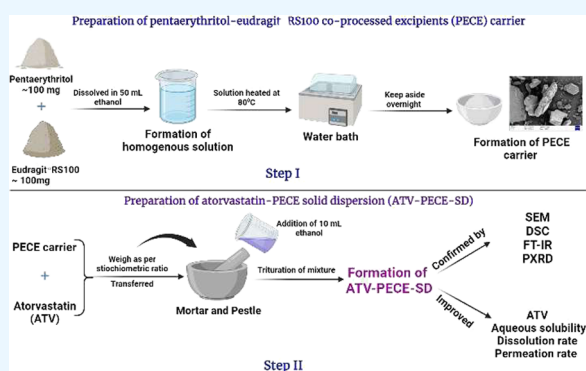
1. INTRODUCTION

Atorvastatin (ATV) (IUPAC name: (3*R*,5*R*)-7-[2-(4-fluorophenyl)-3-phenyl-4-(phenyl carbamoyl)-5-(propan-2-yl)-1*H*-pyrrol-1-yl]-3,5-dihydroxyheptanoic acid) HMG-CoA reductase enzyme inhibitor reduces the cholesterol production by preventing HMG-CoA conversion to mevalonate.[1] Despite these encouraging health benefits, ATV has a low oral bioavailability of about ∼12%, which could be attributed to its poor water solubility of ∼0.1 mg/mL, extensive first-pass metabolism, crystalline behavior, and short half-life of ∼1−2 h, respectively.[2] Due to its limited water solubility and high intestinal permeability profile, ATV is categorized as a biopharmaceutical class II drug. According to reports, ATV poor water solubility and shorter half-life cause an increase in dose, and serious side effects include arthralgia, rhabdomyolysis, liver problems, and renal failure.[3] Therefore, we synthesized and developed a solid dispersion carrier with the

goal to enhance the poor water solubility, permeability, and other biopharmaceutical attributes of ATV.

Many formulation approaches have been reported to enhance the ATV solubility, permeability, and dissolution rate. These include tablets,[4] solid dispersion,[1] nano-solid dispersion,[5] semi-solid binary systems,[6,7] nanocrystals,[8] and binary and ternary solid dispersion.[9] A comprehensive examination of different formulation techniques revealed a small improvement in the biopharmaceutical properties of ATV but with many shortcomings. For instance, neem gum-based solid dispersion of ATV improved its limited aqueous
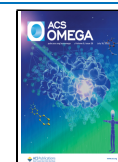
solubility by ~3-fold and ~4-fold compared to pure ATV.[1] The electrospinning approach had a significant impact on a nano-solid dispersion of ATV/ezetimibe with PVP K30 at a ratio of (1:1 and 1:5). This study focused on a few physicochemical assessments without looking into ATV aqueous solubility, permeability, and oral bioavailability.[5] The development of ATV semi-solid dispersion utilizing Gelucire 44/14 and 50/13 simply improved the absorption and half-life of ATV without assessing its formulation stability.[6] ATV solid dispersion with polyethylene glycol 4000 and 10,000 has also been reported to impart high viscosity and significant toxicity to the formulations.[10] According to reports, poloxamer-based solid dispersion can cause particle aggregation and structural changes in the formulation under varied temperatures and concentrations.[11] The observed shortcomings and noneffectiveness of the existing formulations guide us to develop the co-processed excipients as solid dispersion carriers with enhanced ATV water solubility, permeability, and dissolution rate.

Co-processed excipients are multifunctional excipients created by combining two or more existing excipients at the subparticle level, resulting in a single composite excipient with greater functionality when compared to a physical mixing of the same excipient combination.[12] It improved flow properties, compressibility, dilution potential, disintegration properties, and reduced lubrication sensitivity. Together with these benefits, co-processed excipients have also been reported to enhance the solubility, wettability, stability, and gelling properties of food ingredients, excipients, and active pharmaceutical ingredients.[13] Due to these advantages, researchers have been more interested in using co-processed excipients as solid dispersion carriers to improve the biopharmaceutical characteristics of drugs that are weakly water soluble. The solid dispersion formulation remarkably improved the solubility, permeability, dissolution, and pharmacokinetic profile of poorly aqueous soluble drugs[14−16] by reduction of drug particle size to submicron particles, changing the crystalline state to high-energy amorphous state, and improving the wettability, solubility, and dissolution rate of the drug.[17] Previous reports have shown the use of co-processed excipients as solid dispersion carriers with an enhanced dissolution rate of glimepiride, a poorly water-soluble drug.[18] Pentaerythritol-EudragitRS100 co-processed excipients (PECE) were investigated in the current study as potential solid dispersion carriers for improved ATV solubility, permeability, and dissolving rate. The PECE carrier, in association with the solvent evaporation method, converts the crystalline ATV particles into high-energy state amorphous powder, which increases the drug particle solubility and dissolution rate due to an increase in the surface area. Pentaerythritol is a crystalline, highly aqueous soluble ~56 mg/mL compound with molecular formula $C_5H_{12}O_4$. Pentaerythritol offers maximum encapsulation and accommodation to all crystalline molecules due to its structural similarity and low lattice energy. This mechanism of pentaerythritol improved the solubility and dissolution rate of the drug through its dispersion and partial or complete amorphization.[19] EudragitRS100 (ERS100) is a cationic copolymer. The presence of ~4.5−6.8% of functional quaternary ammonium groups on this polymer creates strong intermolecular interaction with a negative drug charge. This interaction improved the drug encapsulation within the polymer and resulted in the formation of a drug−copolymer complex, which allows for controlled,

prolonged, and localized drug delivery.[20] Pentaerythritol and copolymer have the ability to deliver drugs, but their combined and therapeutic uses as solid dispersion carriers have not been fully investigated. Research groups of Chiou et al. and Barzegar-Jalali et al.[21,22] have given a few publications on using pentaerythritol and copolymer as solid dispersion carriers. These studies, however, lacked a thorough and systematic physicochemical and functional characterization of formulations. Therefore, the PECE carrier was prepared, and its feasibility as a solid dispersion carrier was explored. The carrier was synthesized via chemical interaction (i.e., ion-pair and hydrogen bonding) between 5% quaternary ammonium groups of copolymer and hydroxyl groups of pentaerythritol in the presence of ethanol. This interaction further improved the accommodation of the amorphous copolymer within the crystal lattice of pentaerythritol and resulted in the formation of a PECE carrier with high dominance of pentaerythritol. The PECE carrier, which contains 5% quaternary ammonium and hydroxyl groups of copolymers and pentaerythritol, may produce strong electrostatic interactions with the COOH, N−H, and O−H groups of ATV in solid dispersion formulations. This interaction facilitated the accommodation of highly crystalline ATV within the crystal lattice of pentaerythritol, resulting in complete amorphization and the formation of molecular dispersion with enhanced ATV solubility and dissolution rate.

This is a "proof-of-concept" study that intends to investigate the feasibility of PECE as a solid dispersion carrier to improve the ATV aqueous solubility, permeability, and dissolution rate. This work was carried out in two steps. First, the PECE carrier was synthesized using the solvent evaporation method, and then the PECE-based solid dispersion of ATV was developed using the same methodology. The particle size, Fourier transforms infrared spectrophotometry, scanning electron microscopy, differential scanning calorimetry, solubility analysis, and in vitro dissolution studies were used to evaluate the optimized formulations. Also, the same formulations were evaluated for preliminary stability studies under temperature and relative humidity conditions.

2. RESULTS AND DISCUSSION

2.1. Preparation of PECE and ATV-PECE-SD. The PECE carrier was prepared using a combination of pentaerythritol and ERS100 via ethanol-based solvent evaporation method. The ERS100 bearing 5% functional quaternary ammonium groups has chemically interacted with hydroxyl groups of pentaerythritol in the presence of ethanol. This interaction facilitates the easy accommodation and encapsulation of amorphous ERS100 within the crystal lattice structure of pentaerythritol, resulting in the development of a PECE carrier with a high dominance of pentaerythritol, as seen in physicochemical characterization studies. ATV demonstrates low water and higher organic solvent solubility.[23] This physicochemical property of ATV was utilized further to prepare its solid dispersion using the solvent evaporation method. Previous studies have reported the use of water[1] and methanol[24] as the choice of solvents for developing ATV solid dispersion. We tried these solvents to prepare an ATV solid dispersion using a PECE carrier. However, the ATV and PECE exhibit low solubility and dissolution in the water due to their precipitation. In methanol, the ATV shows good solubility, but the PECE carrier displays low solubility and dissolution due to their precipitation. The precipitation issue was solved by
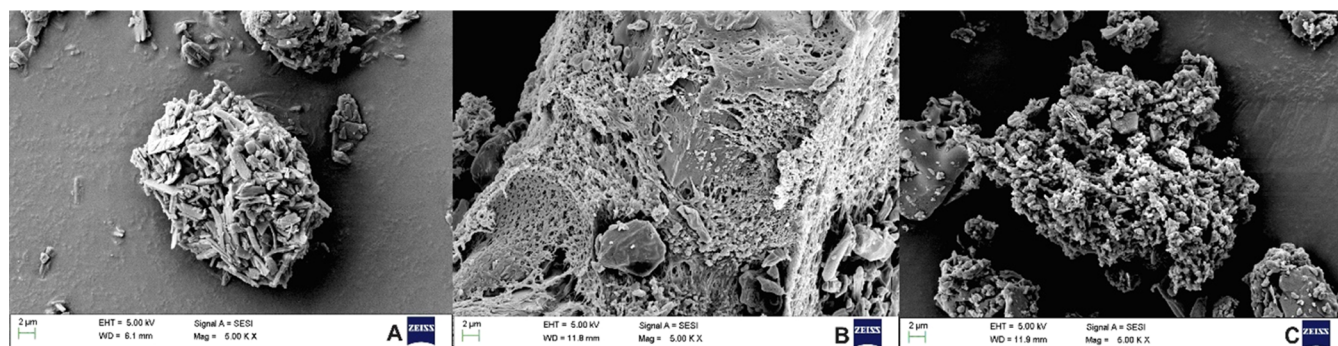
**Figure 1.** SEM images of (A) ATV, (B) PECE carrier, and (C) optimized ATV-PECE-SD3 (1:4) formulations.

exploring other solvents, including acetone, 1,4-dioxane, and absolute ethanol. The ATV and carrier had the same solubility issues as in acetone and 1,4-dioxane, as they did in water and methanol. Apart from the solubility issue, the 1,4-dioxane solvent reported toxicity profile in humans restricts its use in the preparation of solid dispersion. Finally, the absolute ethanol displayed fair solubility and dissolution for both components, resulting in the formation of an amorphous ATV-PECE-SD. The enhanced solubility might be attributable to the formation of hydrogen bonds between the ethanol, ATV, and PECE carrier, which could enhance component solubility and dissolution, resulting in an amorphous ATV solid dispersion. The physicochemical properties of ethanol, including its low toxicity profile, class III solvent, and semi-polar nature, could also contribute to the formation of hydrogen bonding between solvent and ingredients, producing amorphous solid dispersion and improving their solubilization and dissolution. Moreover, the PECE carrier encompassing functional quaternary ammonium and hydroxyl groups electrostatically interacted with COOH, N−H, and O−H groups of ATV. This interaction facilitates the accommodation of highly crystalline ATV within the crystal lattice structure of pentaerythritol, causing its complete amorphization and the formation of molecular dispersion with enhanced solubility and dissolution rate of ATV.

2.2. Particle Size and Zeta Potential Analysis. Particle size distribution offers physical stability and effective drug release performance from formulations. The particle size and zeta potential results of ATV-PECE-SD3 (1:4) are discussed below. The ATV-PECE-SD3 (1:4) formulations showed an average particle size of ∼477.77 nm. The submicron particles in the range of ∼50−1000 nm improved the solubility and dissolution rate of BCS class II drugs.[25] In contrast, the particle size of the studied solid dispersion was similarly in the same range, showing that the formulation was suitable for the oral route. Additionally, most pharmaceutical excipient's particle sizes are inversely proportional to their surface area/volume ratio (SA/V).[26] The smaller particle size of the solid dispersion formulations also displays a larger surface area/volume ratio, which improves ATV solubility and dissolution rate. It could be attributed to trituration, suggesting that the continuous trituration process can reduce the ATV and carrier particle sizes to a great extent, increasing their interaction with each other and thus improving the ATV solubility. The structural similarity and low lattice energy of the PECE carrier could accommodate the ATV particle within the carrier. Interaction caused significant amorphization and produced smaller ATV solid dispersion particle sizes.[21] The formulation also exhibits a

lower polydispersity index value of ∼0.26 (<0.3), indicating a narrow particle size distribution of ATV solid dispersion. Zeta potential is used to measure the strength of charge particles dispersed in a liquid medium. The ATV-PECE-SD3 (1:4) formulations exhibit a zeta potential value of ∼−13.06 mV. The value appeared to be in close agreement with earlier published reports indicating that a value of more than ± 10 mV provides better physical stability for the formulations.[27] According to the results, smaller particle size, polydispersity index, and zeta potential are appropriate for enhancing ATV solid dispersion physical stability.

2.3. Scanning Electron Microscopy (SEM) Studies. SEM offers information regarding the microstructure and surface morphology of the formulation components. The images of pure ATV, PECE carrier, and ATV-PECE-SD3 (1:4) formulations are depicted in Figure 1A−C. Figure 1A shows the images of pure ATV. Particles appeared as bunches of small and large needle shape particles with irregular and ill-defined morphology. The rough, heterogeneous, and porous surface morphology of the PECE carrier (Figure 1B) indicated pentaerythritol and ERS100 interaction in the presence of ethanol, which could form a rough and porous surface carrier. Compared to this, the images of ATV-PECE-SD3 (1:4) formulations (Figure 1C) shows a porous surface with irregular shape characteristics, indicating ATV needle-shaped particles entrapped within the porous surface of the carrier. It also suggests that the triturated-assisted reduced ATV particles may entrap within the porous space of the carrier, creating significant interaction between them and resulting in the development of amorphous solid dispersion. Moreover, the solvent evaporation method could also assist in the development of ATV amorphous solid dispersion.

2.4. Fourier Transform Infrared (FT-IR) Analysis. The FT-IR confirms the formation of solid dispersion by detecting the molecular level interaction between the drug functional groups and polymers. The spectra of pure ATV, pentaerythritol, ERS100, PM3 (1:4), PECE carrier, and optimized ATV-PECE-SD3 (1:4) formulations are displayed in Figure 2, respectively. The pure ATV spectrum exhibits absorption peaks at ∼3675.2 and 3213.0 cm^{-1} for the free hydroxyl and bounded groups (O−H stretching), 3362.1 cm^{-1} for the amide (N−H stretching), and 2970.7 cm^{-1} for the aromatic groups (C−H stretching). There are also peaks at 1649.2 cm^{-1} for keto-amide (C═O stretching), 1580.4 cm^{-1} for amide (N−H bending), 1435.0 cm^{-1} for (C−C stretching), and 1315.8 cm^{-1} for pyrrole (C-N stretching). Peaks are consistent with those of ATV published earlier.[28,29] The FT-IR spectrum of pentaerythritol shows the absorption peaks at ∼3302.4 cm^{-1} for O−H
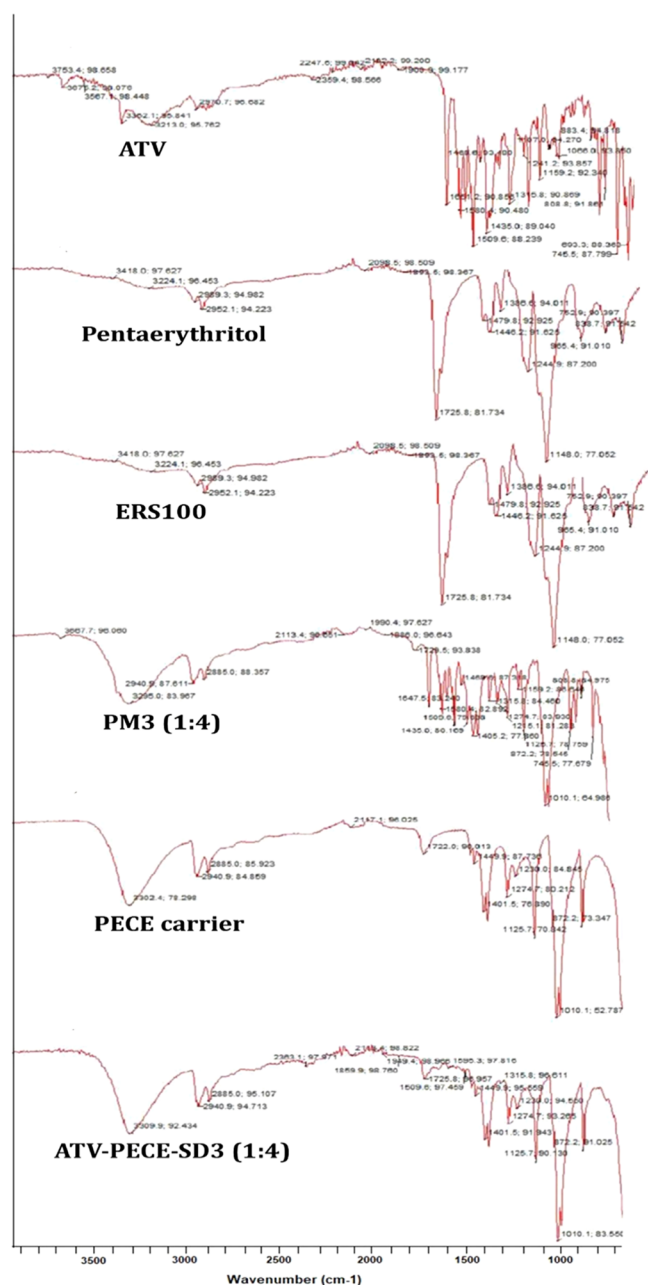
Figure 2. FT-IR spectra of ATV, pentaerythritol, ERS100, PM3 (1:4), PECE carrier, and optimized ATV-PECE-SD3 (1:4) formulations.

stretching, 2940.0 and 2885.0 cm^{-1} for asymmetric C−H stretching, 1230.0 and 1125.7 cm^{-1} for C−C stretching, and 1010.1 cm^{-1} for C = O stretching frequency.[30] The ERS100 spectrum displayed the peaks at ~3418.0 and 3224.1 cm^{-1} for O−H and N−H stretching, respectively, 2989.3 and 2952.1 cm^{-1} for C−H stretching, 1725.8 cm^{-1} for C≡O stretching, and 1479.8 and 1446.2 cm^{-1} for C−C stretching. Also, the peak appeared at ~1386.8 cm^{-1} for N−O stretching due to the presence of the nitro group, whereas the peak was observed at ~1241.9 cm^{-1} for C−O stretching and 1148.0 cm^{-1} for C−H stretching due to the presence of alkyl halide.[20] The FT-IR spectrum of PM3 (1:4) exhibits additive peaks corresponding to pentaerythritol, ERS100, and pure ATV. The FT-IR spectrum of the PECE carrier demonstrated the dominance of pentaerythritol peaks with the appearance of an ERS100 low-intensity peak at 1722.0 cm^{-1} for C≡O stretching. It

indicates that the ERS100 interacted with carbonyl groups of pentaerythritol. This interaction caused the inclusion of this peak within pentaerythritol, leading to the formation of the PECE spectrum. The ERS100 peaks at ~3418.0 cm^{-1} and 3224.1 cm^{-1} (for O−H and N−H stretching) also interacted with O−H groups of pentaerythritol due to the electrostatic interaction, showing the merging and broadening of O−H peaks compared to original one indicating PECE formation.[31] Finally, the ATV-PECE-SD3 (1:4) exhibits a spectrum similar to that of the PECE carrier and pentaerythritol with the appearance of new and retention of old peaks. The high-intensity new peak that appeared at ~3309.9 cm^{-1} was actually shifted from the low-intensity peak at ~3302.4 cm^{-1}. It could be attributed to the strong interaction of O−H groups of pentaerythritol with O−H and N−H groups of ATV and ERS100, respectively, due to intermolecular interaction (*i.e.*, hydrogen bonding, ion−dipole, and van der Waals forces). Forces caused the merging of these functional groups, resulting in a high-intensity and broad absorption peak at ~3309.9 cm^{-1}. Moreover, the spectrum shows the retention of ATV and ERS100 peaks at the lower frequency region, indicating no interaction between the ATV, polymer, and carrier. Spectrum comparison suggests that the development of intermolecular interaction between O−H and N−H groups of ATV, polymer, and PECE carriers could be the primary reason for the formation of solid dispersion.

2.5. Differential Scanning Calorimetry (DSC) Studies. The DSC analyzed the qualitative and quantitative solid-state interactions between the formulation ingredients. These interactions are demonstrated by the development and absence of sharp, small, and diffuse endothermic peaks as a function of temperature. The pure ATV, pentaerythritol, PM3 (1:4), PECE carrier, and ATV-PECE-SD3 (1:4) thermograms are shown in Figure 3. The pure ATV thermogram shows two small endothermic peaks. The first peak observed at ~132.7 °C was likely attributed to dehydration, while the second peak at ~158.43 °C was ascribed to the melting point.[24] Pentaerythritol exhibits two endothermic peaks. The first peak at ~196 °C was possibly attributed to its phase transition pattern from its tetragonal form (crystal structure II) to cubic form (crystal structure I). The second broad and diffuse peak at ~281.5 °C elucidates its melting point.[21,32] The PM3 (1:4) revealed the additive peaks between the range of ~87.86−268.94 °C, indicating the presence of ERS100, pure ATV, and pentaerythritol, respectively. Despite these peaks, the ATV displayed a peak shift to ~116.98 °C compared to the original ATV peaks, indicating ATV interaction with both polymers. Moreover, the lower amount of ATV within the PM prevented detection at the appropriate temperature, leading to lower intensity peaks. Compared to ATV, the ERS100 and pentaerythritol peaks were also shifted compared to their original peaks, suggesting the development of an *in situ* mixture. At the same time, the increasing temperature may also induce the encapsulation of ATV and ERS100 within the crystal lattice structure of pentaerythritol, leading to the formation of PM with low-intensity peaks. The PECE carrier displays a thermogram similar to that of pentaerythritol but with shifted peak intensity and position to a low-intensity peak at ~197.59 and ~255.23 °C, respectively, compared to the original peaks of pentaerythritol and ERS100, indicating significant interaction between them. The disappearance of the ERS100 peak and the shifting of the pentaerythritol two peaks could be attributed to the low-lattice energy crystal
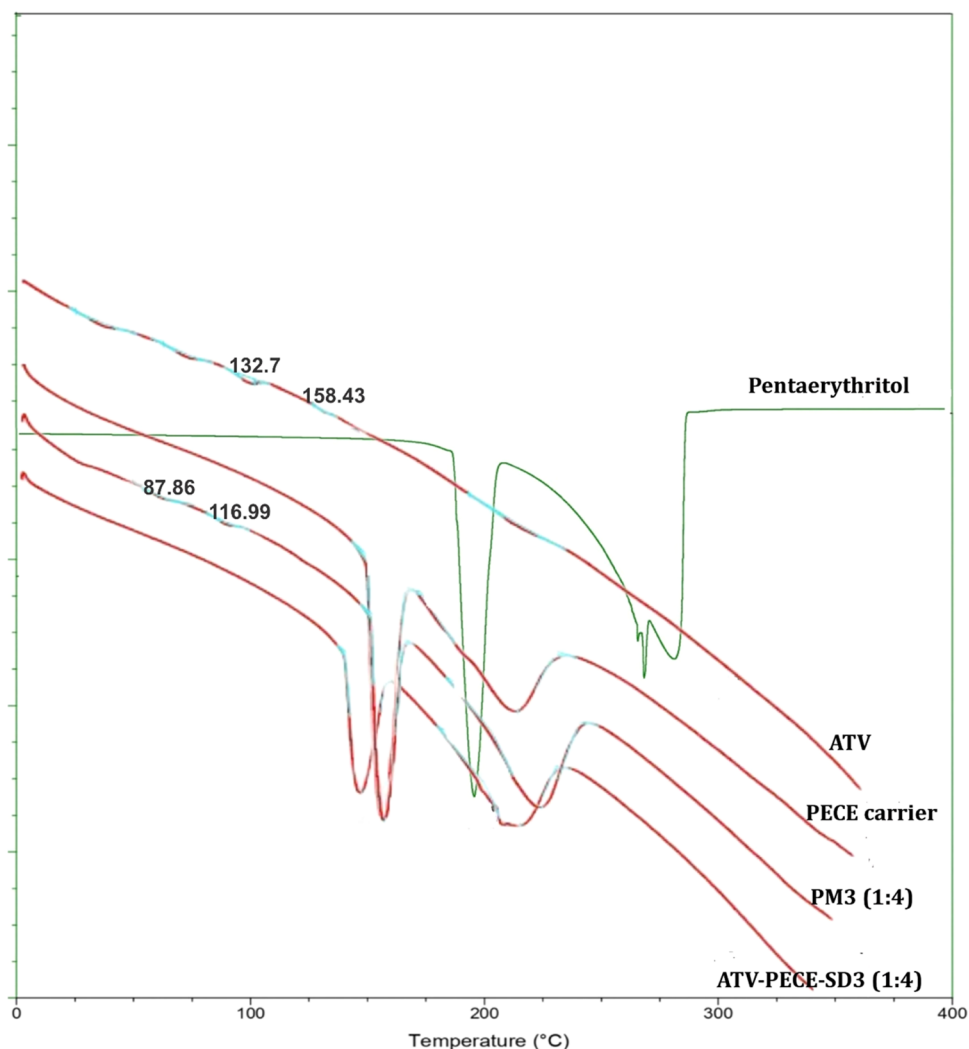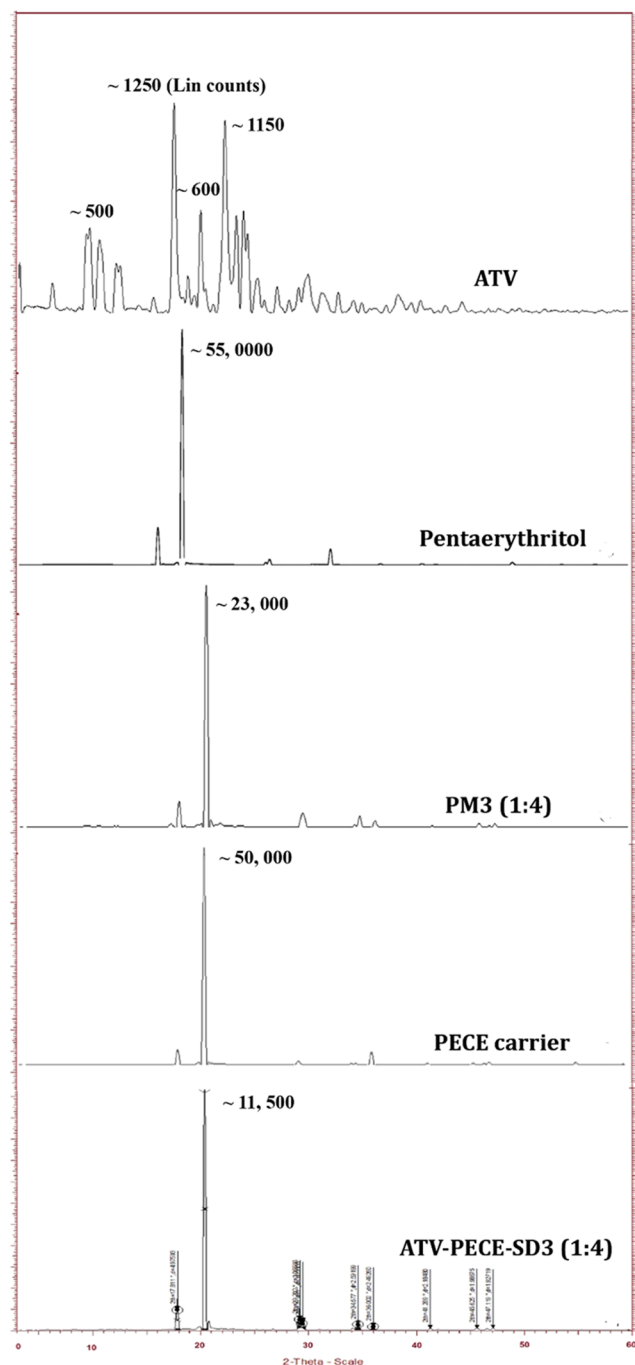
Figure 3. DSC thermograms of ATV, pentaerythritol, PM3 (1:4), PECE carrier, and optimized ATV-PECE-SD3 (1:4) formulations.

structure of pentaerythritol, which accommodates and merges the ERS100 diffused peaks into pentaerythritol. This explanation provides evidence of carrier formation with the dominance of pentaerythritol thermograms.[21,32] The thermograms of ATV-PECE-SD3 (1:4) revealed two characteristic peaks. First, the complete absence of ATV peaks; second, thermograms show similarity to pentaerythritol with two different peak positions and intensities around ~198.2 and 269.22 °C, respectively. It indicates that the carrier was positively associated with ATV and formed an amorphized solid dispersion. This phenomenon suggests that the PECE carrier containing phase transition behavior of pentaerythritol around ~23 cal/degree/mole dominance could be able to accommodate crystalline ATV particles within its crystal lattice, allowing their dispersion, amorphization, and subsequent formation of amorphous solid dispersion.[21] The thermal changes in comparison to the original peaks confirm the development of solid dispersion.

2.6. Powder X-ray Diffraction (PXRD) Studies. Typically, PXRD examines changes in the API crystalline pattern. Figure 4 displays the diffractograms of pure ATV, pentaerythritol, PM3 (1:4), PECE carrier, and ATV-PECE-SD3 (1:4) formulations. Pure ATV shows the sharp and intense diffraction peaks on the 2θ scale at a position of ~17°

(~1250 Lin counts), 20° (~600), 22° (~1150), 23° (~600), and 24° (~600), respectively. It also displayed broad and diffuse peaks at ~3, 6, 9, 10, 12, and 25°, indicating ATV crystalline nature. Peaks are consistent with earlier published literature.[33] Pentaerythritol showed a single sharp promising peak at ~20° (~55,0000 Lin counts) and three diffuse peaks at ~18, 29, and 36°, indicating a pentaerythritol crystal lattice structure.[21] PM3 (1:4) diffractograms show intense and tiny diffuse peaks corresponding to pentaerythritol and ERS100. Pentaerythritol peak patterns are the same as in the original, except for low-intensity peaks at ~20° (~23,000 Lin counts). However, some representative peaks of ERS100 were found between the region of ~40−60°, indicating the polymer's amorphous nature. The findings are well supported by earlier published literature.[34] The spectrum exhibits the diffraction peaks of the PECE carrier. It displayed the pentaerythritol diffraction pattern with low-intensity peak characteristics compared to the original one. Some miniature diffused peaks were found between ~40 and 60° that showed partial merging into the pentaerythritol diffraction peaks, indicating the contribution of polymers to the carrier synthesis. The formation of the carrier peak suggests that pentaerythritol encapsulates the polymer within its crystal lattice structure, causing dispersion, amorphization, and merging of polymer

Figure 4. PXRD of ATV, pentaerythritol, PM3 (1:4), PECE carrier, and optimized ATV-PECE-SD3 (1:4) formulations.

solid dispersion with high surface area characteristics and completes ATV dispersion and amorphization. Results conclude that the carrier successfully produced the solid dispersion formulation and reduced the ATV crystalline status (Table 1).

Table 1. Composition of the ATV-PECE-SD Formulations[a]

formulations	ATV (mg)	PECE carrier (mg)
ATV-PECE-SD1	40	50
ATV-PECE-SD2	40	100
ATV-PECE-SD3	40	200
ATV-PECE-SD4	40	300
ATV-PECE-SD5	40	400

[a]ATV-PECE-SD, atorvastatin-pentaerythritol-eudragitRS100 co-processed excipient-solid dispersion; ATV, Atorvastatin; and PECE, -pentaerythritol-eudragitRS100 co-processed excipients.

2.7. Drug Content Analysis. The ATV content within solid dispersion formulations is shown in Table 2. The carrier-

Table 2. Drug Content of ATV in ATV-PECE-SD Formulations[a]

formulations	drug content (%, w/w)[b]
ATV-PECE-SD1	96.94 ± 1.12
ATV-PECE-SD2	97.85 ± 1.01
ATV-PECE-SD3	98.35 ± 1.07
ATV-PECE-SD4	96.24 ± 0.98
ATV-PECE-SD5	96.59 ± 1.23

[a]ATV-PECE-SD, atorvastatin-pentaerythritol-eudragitRS100 co-processed excipient-solid dispersion. [b]Data represents the mean value of 3 replications ± standard deviation.

based solid dispersions, i.e., ATV-PECE-SD1 (1:1), ATV-PECE-SD2 (1:2), ATV-PECE-SD3 (1:4), ATV-PECE-SD4 (1:6), and ATV-PECE-SD5 (1:8), showed the ATV content around ∼96.94, 97.85, 98.35, 96.24, and 96.59% w/w, respectively. Compared to all, the ATV-PECE-SD3 formulations at the drug and carrier ratio (1:4) exhibit a higher drug content of around ∼98.35 ± 1.07% w/w, indicating better interaction and association between the drug and the carrier. Based on this, the ATV-PECE-SD3 (1:4) formulations are considered optimized formulations for further characterization studies. The ATV-PECE-SD3 formulation (1:4) ratio with a drug content of 98.35% w/w suggests that the carrier in support of the solvent evaporation method could increase the drug dispersion, interaction, and subsequent incorporation within the carrier matrix, reducing the variability between the replicates and increasing the drug content in the solid dispersion.[10]

2.8. Saturation Solubility Studies. Table 3 exhibits the aqueous solubility analysis of pure ATV, PM, and ATV-PECE-SD formulations. As shown in the table, pure ATV has a low aqueous solubility of ∼0.17 mg/mL, indicating that it is a BCS class II (i.e., low solubility and high permeability) drug, resulting in low oral bioavailability.[2] The physical mixture with increasing carrier ratios improved the drug's modest aqueous solubility from ∼0.27 to 1.64 mg/mL. The PM1, PM2, and PM3 had a drug-to-carrier ratio of (1:1), (1:2), and (1:4), respectively, which enhanced the aqueous drug solubility by ∼10-fold. However, the PM4 (1:6) and PM5 (1:8) lowered the aqueous drug solubility, and their level of significance is

peaks into pentaerythritol and shifting its peak position to a low-intensity peak at ∼20° (∼50,000 Lin counts) compared to original peaks. The ATV-PECE-SD3 (1:4) formulations displayed the absence of ATV crystalline peaks with the appearance of pentaerythritol low-intensity peaks at ∼20° (∼11,500 Lin counts) compared to the original drug and carrier peaks. It shows that the carrier and ATV successfully interacted in the presence of ethanol, resulting in the production of an amorphized solid dispersion. This mechanism suggests that the multifunctional carrier with pentaerythritol dominance could accommodate the entire crystalline ATV particle within its crystal lattice due to its structural similarity with the drug. This interaction results in the formation of a

Table 3. Solubility Data of Pure ATV, the Physical Mixture (PM) of Pure ATV and PECE Carrier, and ATV-PECE-SD Formulations[a]

formulations	aqueous solubility (mg/mL)[b]
pure ATV	0.17 ± 0.07
PM1	0.27 ± 0.04
PM2	0.39 ± 0.05
PM3	1.64 ± 0.03
PM4	1.31 ± 0.09
PM5	1.20 ± 0.04
ATV-PECE-SD1	2.78 ± 0.12
ATV-PECE-SD2	4.45 ± 1.09
ATV-PECE-SD3	7.23 ± 1.20
ATV-PECE-SD4	6.14 ± 0.16
ATV-PECE-SD5	5.87 ± 0.08

[a]Pure ATV, pure atorvastatin; PM, physical mixture; and ATV-PECE-SD, atorvastatin-pentaerythritol-eudragitRS100 co-processed excipients solid dispersion. [b]Data represents the mean value of 3 replications ± standard deviation.
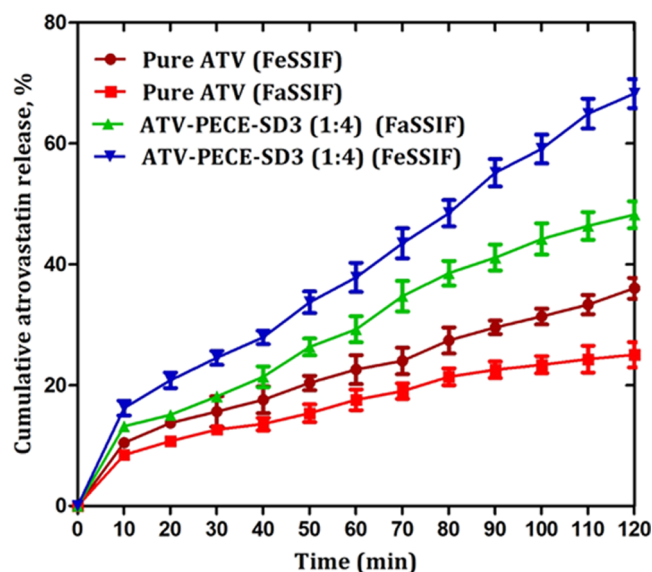

Figure 5. *In vitro* drug dissolution profiles of ATV from pure ATV, PM3 (1:4), and optimized ATV-PECE-SD3 (1:4) formulations, respectively. Data represents the mean value of 3 replications ± standard deviation.

nonsignificant compared to pure ATV. Results suggest that higher carrier concentrations may restrict the drug's contact with the aqueous media and reduce its aqueous solubility. Moreover, PM1, PM2, and PM3 enhanced aqueous drug solubility. It might be explained by the close association and subsequent interaction of highly water-soluble carriers with drug particles, which led to the drug's partial amorphization and increased aqueous solubility. The solid dispersion formulations improved the drug's aqueous solubility compared to the pure drug and physical mixture. Compared to all SDs, the optimized ATV-PECE-SD3 (1:4) formulations improved the aqueous drug solubility by ~43-fold. This value was ~7.23 mg/mL. The statistical data for the saturation solubility studies demonstrated a *p*-value less than 0.0001. The experimental observations for all eleven data sets show that the term was significant for the respective statistical model. In contrast, the F and R squared values were ~83.47 and 0.9743, respectively, representing the significance of the data after applying one-way ANOVA. The PM3 solubility value exhibited statistical significance ($p < 0.05$) compared to pure ATV. All solid dispersion formulation solubility values also demonstrated statistical significance ($p < 0.0001$) compared to pure ATV. The ATV-PECE-SD1, ATV-PECE-SD2, ATV-PECE-SD4, and ATV-PECE-SD5 also improved the ATV solubility, indicating that the carrier significantly improved the drug solubility. This phenomenon suggests that the carrier contains the structurally similar and low lattice energy of pentaerythritol, which accommodates the entire drug particle within its crystal lattice and establishes weak interaction forces. This interaction results in the amorphization of ATV particles and produces an amorphous solid dispersion with high solubility characteristics.[35,36] It also implies that the amorphization and solvation impact of amorphous polymers on ATV particles could increase their water solubility through weak electrostatic interactions.[22]

2.9. Dissolution Studies. *In vitro* dissolution is employed to assess the rate of drug release from the pharmaceutical dosage form. Figure 5 displays the comparative release performance of ATV from pure ATV, PM3 (1:4), or optimized ATV-PECE-SD3 (1:4) formulations. The figure shows that by the end of 120 min, pure ATV showed only ~29% dissolution in phosphate buffer, indicating that the drug has poor aqueous
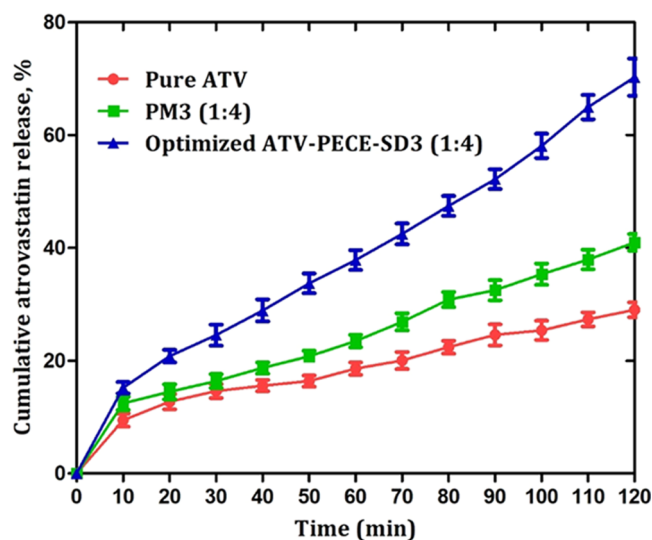
solubility. PM3 (1:4) produced a higher ATV dissolution rate than pure ATV. The PM followed the same dissolution pattern as pure ATV and released the drug at around ~23% by the end of 60 min. However, after this period, the PM increased drug dissolution by ~41%, and their value was nonsignificant when compared to pure ATV, implying that the hydrophilic nature of pentaerythritol and the polymer may form a close association with the drug particles, causing partial amorphization, and thus increasing the drug dissolution. Compared to the pure drug, the optimized ATV-PECE-SD3 (1:4) significantly improved the drug dissolution performance. The optimized formulations exhibited ~38% drug dissolution at 60 min. After this period, the drug dissolution reached a maximum level of ~70%, indicating that the highly soluble carrier improves the drug dissolution. After applying one-way ANOVA, the *p*-value for the *in vitro* dissolution study was found to be 0.0034, which stated that the significant results obtained during the study as this value is less than 0.05. The F and R squared value also support the important observations obtained during the study protocol, which were ~6.694 and 0.2711, respectively. Moreover, Bartlett's test for equal variance demonstrated the same significance level with a *p*-value of 0.0034, less than 0.05. When Dunnett's multiple comparison tests were employed to combine different formulations vs the ATV encapsulated solid dispersions (ATV-PECE-SD3), the value of t was found to be at 3.553 for pure ATV and 2.534 for PM3. The optimized ATV-PECE-SD3 formulation dissolution data shows more statistical significance ($p < 0.01$) compared to pure ATV and less significant ($p < 0.05$) compared to PM3. Findings indicate that combining a solvent evaporation method with a synthesized carrier, individual pentaerythritol, polymer, and ethanol solvent could enhance the ATV dissolution performance in the dissolution media. The well-established solvent evaporation technique converts the highly crystalline ATV particles into high-energy state amorphized particles, facilitates their solubilization, and enhances dissolution.[37] The hydrophilic carrier develops the association and interaction with the O−H, N−H, and carboxyl groups of the drug. This association may increase the drug dispersion

within the carrier and improve its dissolution to a great extent. It may also be hypothesized that the presence of 5% functional quaternary ammonium groups of polymers in the carrier creates strong electrostatic interaction with the carboxylic groups of the drug, resulting in partial amorphization. After that, the pentaerythritol also establishes hydrogen bonding, an ion–dipole, and van der Waals forces with the O–H and N–H groups of drugs. The combined interaction of polymer and pentaerythritol with the drug facilitates the easy accommodation of highly crystalline drugs within the crystal lattice structure of pentaerythritol. It causes their complete amorphization and the formation of molecular dispersion with an enhanced drug dissolution rate. Moreover, the polymer protonation of acidic groups of the drug may also be the reason for increasing the drug dissolution rate.[38] Another explanation suggests that the lower amount of polymer in the carrier may reduce the burst effect of the drug and hence increase its dissolution.[39] Like other hydrophilic carriers, the synthesized carrier may also inhibit nucleation and crystal growth, prevent the reprecipitation of an amorphized drug from a supersaturated solution, and enhance the drug dissolution rate.[40] Because of ethanol's semi-polar nature and hydrogen bonding formation capacity, it might establish hydrogen bonds with the drug and the carrier, resulting in improved drug solubilization and subsequent dissolution. Changes in the physicochemical properties of drugs and carriers as a result of their chemical interaction may also improve the drug dissolution rate.[41]

2.10. DE Studies. The DE results are discussed below. The pure ATV exhibits a lower value of ~10.02 ± 1.63%. The PM (1:4) shows a modest value of ~28.43 ± 1.12%. In contrast, the optimized ATV-PECE-SD3 (1:4) formulations demonstrated higher values around ~61.18 ± 2.08%, indicating that optimized formulations enhanced the dissolution efficiency values compared to the pure drug and physical mixture. It suggests that improved solubility of the drug by the carrier could be responsible for higher dissolving efficiency values in solid dispersion formulations.

2.11. Fasted vs Fed State Dissolution Comparison Studies. Figure 6 depicts the effect of food intake on the dissolving performance of pure ATV or prepared ATV-PECE-SD3 (1:4) formulations in the fed and fasted states. In fasted conditions, the pure ATV displayed only ~25% dissolution at the end of the testing period. The same drug exhibits a higher rate and extent of dissolution around ~36%. It is indicative that the food content could enhance the solubilization and dissolution of poorly water-soluble drugs. The findings are consistent with earlier published reports.[42] The optimized ATV-PECE-SD3 (1:4) formulations dramatically increased the rate and extent of drug dissolution in fasted and fed states. However, the optimized formulations considerably improved the drug dissolution by ~68% in the fed state as compared to only ~48% drug dissolution in a fasted state. The possible reason behind this is the combined effect of food contents, solubilization, and amorphization of drug particles, resulting in an increase in the dissolution rate in a fed state. Another explanation suggests that the sodium taurocholate, in interaction with the drug and the carrier, forms taurocholate–drug micelles and taurocholate–carrier–drug micelles. The formation of micelles could enhance the drug dispersion, amorphization, solubilization, and dissolution in a fed state as compared to the fasted state.[43] Additionally, the lowest quantities of sodium taurocholate (~1.65 g) and lecithin (~5.9 mL) used in fasted state dissolution media could have


Figure 6. Comparative *in vitro* drug dissolution profiles of pure ATV and optimized ATV-PECE-SD3 (1:4) in fasted and fed states. Data represents the mean value of 3 replications ± standard deviation.

lowered the wetting of pure ATV and ATV-PECE-SD3 solid particles, reducing their solubilization into mixed micelles, thereby lowering their dissolution. Also, the lower buffer capacity and osmolality of the fasted state could also contribute to lower the dissolution of pure ATV and solid dispersion formulations. Whereas the highest quantities of sodium taurocholate (~8.25 g) and lecithin (~29.54 mL) employed in the preparation of fed state dissolution media could facilitate the rapid wetting of pure ATV and solid dispersion particles. Wetting increases the solubilization of pure ATV and optimized ATV-PECE-SD3 formulations into mixed micelles and subsequently enhances their dissolution compared to the fed state. Moreover, the higher buffer capacity and osmolality of the fed state could enhance the dissolution rate of pure ATV and optimize solid dispersion formulations.[42] Findings suggest that the difference in the amount of ingredients used in the preparation of fed and fasted states and their positive interactions with the drug and the carrier could be liable for enhanced drug dissolution in the fed state compared to the fasted state.

2.12. Permeation Studies. Figure 7 depicts the permeation profiles of pure ATV, PM3 (1:4), and ATV-PECE-SD3 (1:4) formulations across the everted rat intestinal membrane. The pure ATV showed only ~27% drug permeation across the intestine, indicating a low permeation profile of the drug. The PM3 (1:4) showed a modest improvement in drug permeation compared to pure drug. It was demonstrated to have around ~23% drug permeation across the membrane at the end of 60 min, and then its permeation profile enhanced and reached ~39% by the end of the 120 min. Their values demonstrate that they are nonsignificant compared to pure drug. This improvement could be attributed to the interaction between the drug and the carrier, and as a result, partial amorphization enhanced drug permeation. The optimized ATV-PECE-SD3 (1:4) formulations enhanced the drug permeation across the biological membrane compared to a pure drug and physical mixture. The optimized formulations permeated ~35% of the drug from the membrane at 60 min. After this, the same formulations
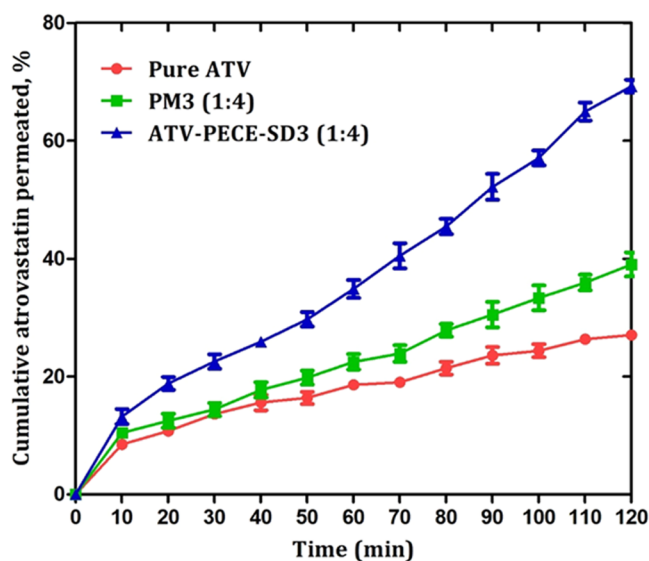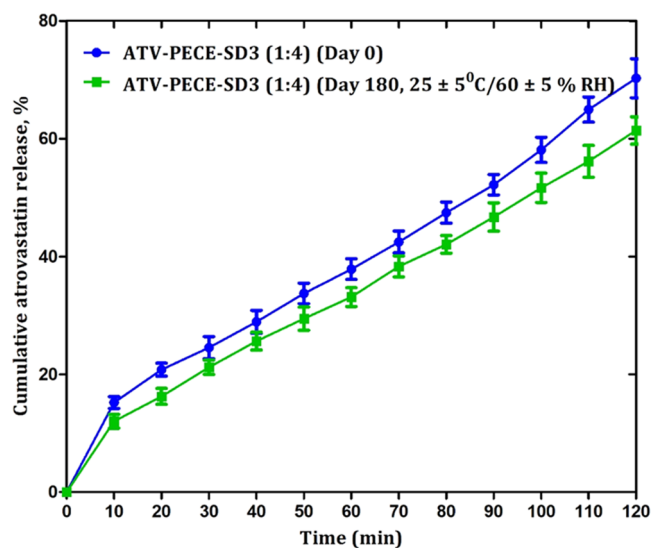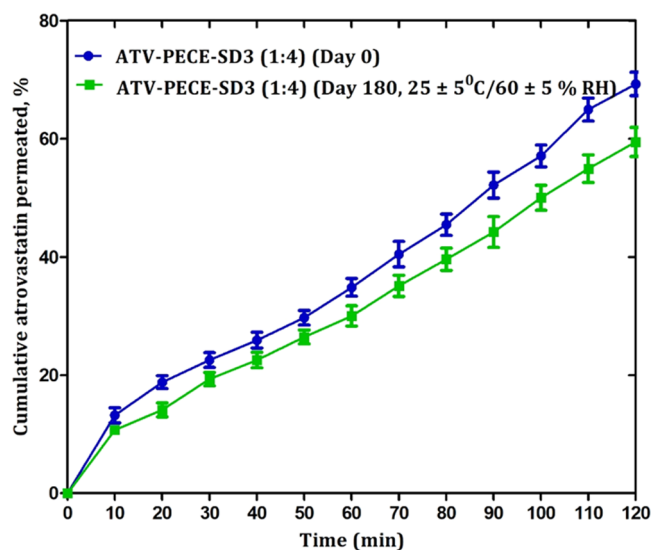
Figure 7. *Ex vivo* drug permeation profiles of ATV from pure ATV, PM3 (1:4), and optimized ATV-PECE-SD3 (1:4) formulations, respectively. Data represents the mean value of 3 replications ± standard deviation.

Figure 8. Comparison of *in vitro* drug dissolution profile of optimized ATV-PECE-SD3 (1:4) before and after 6-month of storage at 25 ± 5 °C/60 ± 5% RH. Data represents the mean value of 3 replications ± standard deviation.

Figure 9. Comparison of *ex vivo* drug permeation profile of optimized ATV-PECE-SD3 (1:4) before and after 6-month of storage at 25 ± 5 °C/60 ± 5% RH. Data represents the mean value of 3 replications ± standard deviation.

enhanced the drug permeation and reached a maximum level of ~69% by the end of the period. After applying one-way ANOVA, the p-value for permeation studies was found to be 0.0046, which stated the significant results obtained during the study as this value is less than 0.05. The F and R squared values also support the significant observations obtained during the study protocol, which were ~6.270 and 0.2583, respectively. Bartlett's test for equal variance demonstrated the same significance level with a p-value of 0.0046, less than 0.05. When Dunnett's multiple comparison tests were employed to compare different formulations vs the ATV encapsulated solid dispersions (ATV-PECE-SD3), the significance of t was found to be 3.404 for pure ATV and 2.548 for PM3. The optimized ATV-PECE-SD3 formulation dissolution data shows more statistical significance ($p < 0.01$) compared to pure ATV and less significant ($p < 0.05$) compared to PM3. It suggests that a developed hydrophilic carrier interacts with the membrane component, potentially improving drug permeation. This effect could be explained by the fact that crystal lattice pentaerythritol and polymer form covalent and noncovalent interactions with the membrane's amphiphilic components. This association may further increase the miscibility of pentaerythritol, a polymer, or a carrier within the amphiphilic component of the membrane, allowing drug particles easy access across the biological membrane.[19,44] Furthermore, encapsulating drug particles within the highly soluble low-lattice energy pentaerythritol may modify the physicochemical properties of the drug and hence improve its permeability.

2.13. Stability Studies. Figures 8 and 9 show the influence of controlled temperature and relative humidity on the dissolution and permeation profiles of ATV from stored optimized ATV-PECE-SD3 (1:4) formulations (at day 180). The stored optimized formulations (at day 180) significantly reduced the drug dissolution by ~61% as compared to the initial formulations (at day 0) by ~70% as shown in Figure 8. The same situation also existed in the *ex vivo* permeation studies, as displayed in Figure 9, in which the stored optimized formulations (at day 180) reduced the drug permeation rate by

around ~59% as compared to the initial formulation drug permeation rate of around ~69% across the biological membrane, indicating that the controlled temperature and relative humidity greatly influenced the dissolution and permeation characteristics of the formulations. It suggests that the relative humidity, external and internal factors could cause substantial changes in the optimized formulation physicochemical properties, resulting in reduced drug dissolution and permeation. The specific explanation behind this is still unclear; therefore, extra physicochemical and functional evaluations are warranted to understand the effect of 6-month storage conditions on solid dispersion.

3. CONCLUSIONS

We successfully synthesized the carrier and investigated its feasibility as a solid dispersion carrier for improving the ATV low water solubility, permeability, and dissolving rate. The PECE carrier formation suggested the involvement of ion-pair and hydrogen bonding between 5% quaternary ammonium groups of the polymer and hydroxyl groups of pentaerythritol. The physicochemical analysis confirmed the formation of solid dispersion formulations due to hydrogen bonding, ion–dipole, and van der Waals forces acting between the COOH, N–H, and O–H groups of ATV and 5% quaternary ammonium and hydroxyl groups of the polymer and the carrier. The optimized formulations enhanced ATV aqueous solubility by around ~43-fold due to the mechanism of accommodation, dispersion, and amorphization as compared to pure ATV and physical mixtures. The optimized formulations significantly enhanced the rate and extent of ATV dissolution as compared to pure ATV. Equally, the results of *ex vivo* permeation studies revealed that optimized formulations enhanced the rate and extent of ATV permeation across the biological membrane compared to pure ATV and PM. The optimized formulations improved the ATV dissolution in the fed state due to the food effect and micelles formation mechanism compared to pure ATV in a fasted state. The preliminary stability studies revealed a lower rate of dissolution and permeation for optimized formulations (at day 180) compared to initial formulations (at day 0) because of relative humidity and other external and internal factors. However, detailed characterization studies must also be conducted to understand the stability mechanism. Hence, the preparation of co-processed excipients using two excipients or polymers could be a potential solid dispersion carrier for improving the delivery of poorly aqueous soluble drugs.

4. MATERIALS AND METHODS

4.1. Materials. ATV of high purity (>99%) was obtained from Alkem Laboratories Ltd. (Mumbai, India). Pentaerythritol was obtained from Sigma-Aldrich Corporation (St. Louis, MO). EudragitRS100 was obtained from Chemsworth Pvt. Ltd. (Bangalore, India). Other chemicals such as calcium chloride, dichloromethane, ethanol, glacial acetic acid, glucose, methanol, n-octanol, potassium chloride, potassium dihydrogen phosphate, sodium chloride, sodium bicarbonate, sodium hydroxide, soya lecithin, and sodium taurocholate were purchased from Loba Chemicals Pvt. Ltd., (Mumbai, India). The purchased chemicals were of analytical grade.

4.2. Preparation of PECE. The solvent evaporation method previously described with a little modification was used to prepare the co-processed excipient (PECE) carrier.[18,31] Briefly, ~100 mg of pentaerythritol and EudragitRS100 (ERS100) were separately weighed. Both ingredients were dissolved in 50 mL of ethanol and stirred well until a homogenous solution was obtained. This solution was heated in a water bath at 80 °C for 15 min. Next, the heated solution was poured into the china dish and kept aside overnight, leading to the formation of PECE powder. This powder was dried at 60 °C in a hot air oven for 2 h. Dried PECE powder was milled using a universal mill at conditions of ~<20,000 RPM, ~7 min run time, ~450 W, ~5–40 °C ambient temperature, and ~230 V (Model: M20, IKA India Pvt., Ltd., Bengaluru, Karnataka, India). The milled materials were sieved using a #60 mesh size to get uniform PECE powder and

preserved in nitrogen-purged amber-colored glass vials until further physicochemical characterization.

4.3. Preparation of ATV-PECE-SD. ATV-PECE-SD was prepared by the solvent evaporation method reported earlier with slight modifications.[45] Briefly, the ATV and PECE carrier were accurately weighed according to stoichiometric ratios (1:1, 1:2, 1:4, 1:6, and 1:8) and transferred into a previously cleaned mortar and pestle. The materials were combined with 10 mL of ethanol, resulting in the formation of a thick paste. This thick paste was triturated continuously until ethanol evaporated, resulting in the formation of ATV-PECE-SD, a porous, dry solid mass. The solid mass was collected and dried at 40 °C in the oven for 24 h. Dried solid dispersion powder was sieved (#60 mesh size) and vacuum dried at 40 °C for 24 h. The dried ATV-PECE-SD powder was transferred into a nitrogen-purged amber-colored (light-resistant) glass vial and stored in a desiccator until further analysis. The composition of the ATV-PECE-SD formulations is summarized in Table 1.

4.4. Preparation of Physical Mixture. As per the ratios (1:1, 1:2, 1:4, 1:6, 1:8), the ATV and PECE carrier were weighed, mixed meticulously, sieved, and then preserved in a nitrogen-purged amber-colored glass vial. A prepared physical mixture was used further for physicochemical and functional characterization studies.

4.5. Particle Size and Zeta Potential Analysis. The particle size and zeta potential are considered the critical parameters of the nanoformulations because they reveal information about the stability and release pattern of the compounds. The particle size and zeta potential of optimized ATV-PECE-SD3 (1:4) formulations were carried out on photon cross-correlation spectroscopy (PCCS) equipped with dynamic light scattering (DLS) technology. The procedure adopted by our group earlier was used in this study.[46] Briefly, ~500 μg/mL aqueous dispersion of optimized ATV-PECE-SD3 (1:4) formulations was prepared and placed in a particle size analyzer chamber (Model: Nanophox Sympatec, GmbH, Clausthal-Zellerfeld, Germany). This dispersion was analyzed, and the results were interpreted using instrument-attached software. The analysis was performed within the sensitivity range of ~1 nm to 10 μm. The aqueous dispersion of optimized formulations was also employed for zeta potential analysis. The sample solution was transferred into the chamber and analyzed within the range of ±200 mV using a nanoparticle analyzer (Model: NanoPlus-2, particulate system, Norcross, GA).

4.6. SEM. The samples of pure ATV, PECE carrier, and optimized ATV-PECE-SD3 (1:4) formulations were analyzed using a scanning electron microscope (Model: Supra55, Carl Zeiss NTS Ltd., Germany). The analysis was performed using the procedure reported earlier.[47] Briefly, ~50 mg of samples were accurately weighed and sprinkled on a double-faced carbon tape. After this, the sample was prepared for microscopic imaging by being coated with a thin layer of gold around ~400° in a sputter coater and scanned at an accelerating voltage of 10 kV. The images were read and interpreted using instrument-attached software (Smart SEM V05.06).

4.7. FT-IR. The functional groups and their interactions between pure ATV, polymer, and formulations were studied using a Fourier transform infrared spectrophotometer (FT-IR). FT-IR (Model: FT-IR-8300, Shimadzu, Kyoto, Japan) was used to investigate samples of pure ATV, pentaerythritol, ERS100, PM3 (1:4), PECE carrier, and optimized ATV-

PECE-SD3 (1:4) formulations. Briefly, the powder mixture of sample and potassium bromide (KBr, FT-IR grade) was prepared using an agate mortar and pestle. This mixture was compressed into thin, transparent discs using a mini hand press machine (Model: MHP-1, P/N-200-66747-91, Shimadzu, Kyoto, Japan). The discs were scanned between 4000 and 400 cm^{-1} and interpreted using FT-IR attached software (control software, version 1.10). The FT-IR procedure reported by our group earlier was used in this study.[48]

4.8. DSC. A DSC was employed to investigate the physical properties and thermal transitions of active pharmaceutical ingredients (APIs) and formulations. The pure ATV, pentaerythritol, PM3 (1:4), PECE carrier, and optimized ATV-PECE-SD3 (1:4) formulations were investigated for their thermal properties using a calibrated differential scanning calorimeter (Model: DSC-1821e, Mettler Toledo AG, Analytical, Schwerzenbach, Switzerland). The DSC analysis was carried out utilizing the methodology previously described by our group.[49] Briefly, ~2 mg of samples were accurately weighed and sealed in an aluminum pan with the lid employing the crimper of the instrument. The samples were heated from 0 to 400 °C at an increment rate of 10 °C/min. Each sample peak transition onset temperature was analyzed and interpreted using instrument-accompanied software (Universal analysis, V4.5A, build 4.5.0.5).

4.9. PXRD. A PXRD instrument was employed to confirm the crystalline and amorphous properties of the formulation components. A PXRD instrument (Model: D8 Advance, Bruker, Inc., Madison, WI) was employed to analyze the samples of pure ATV, pentaerythritol, PM3 (1:4), PECE carrier, and ATV-PECE-SD3 (1:4) formulations. Briefly, ~50 mg of samples were accurately weighed and loaded into the sample analysis area. The samples were irradiated using a radiation source (λ = 1.5406 Å) and detected using a silicon strip-based detector. Each sample diffraction pattern was analyzed and interpreted using instrument-accompanied software. The PXRD procedure reported by our group earlier was used in this study.[50]

4.10. Drug Content Analysis. The ATV content within solid dispersion formulations was analyzed using the method reported earlier in the literature.[10] Briefly, the ATV-PECE-SD formulations (equivalent to ~40 mg of ATV) were accurately weighed and transferred into a 100 mL of volumetric flask. The powder was mixed with freshly prepared 100 mL of phosphate buffer (0.05 M, pH 6.8) using a magnetic stirrer. The dissolved contents were filtered using a membrane filter (0.45 μm), and the filtrate was analyzed for the drug content. An aliquot of the filtrate was diluted and subjected to spectrophotometer analysis for absorbance at a wavelength of about ~246 nm (Model: V-630, Jasco International Co., Ltd., Tokyo, Japan). Additionally, to prevent carrier interference during analysis, a separate carrier solution was also prepared with the same procedure and compared with the sample solution.

4.11. Saturation Solubility Analysis. The solubility analysis of pure ATV, PM, and ATV-PECE-SD formulations was evaluated using the method reported earlier in the literature.[10] Briefly, an additional quantity of the pure ATV, PM, and ATV-PECE-SD formulations were weighed and transferred into 10 mL of screw cap glass vials. These samples were mixed with 10 mL of distilled water using a magnetic stirrer. The vial contents were agitated using a rotary shaker (Model: RS-24 BL, Remi Laboratory Instruments, Remi House, Mumbai, India) at 37 °C for 24 h. The resultant

solution was filtered using a membrane filter (0.45 μm), and the filtrate was collected. An aliquot of the filtrate was diluted and subjected to spectrophotometer analysis (Model: V-630, Jasco International Co., Ltd., Tokyo, Japan) for absorbance at a wavelength of about ~239 nm. The blank solution was used as a comparison for the sample solution.

4.12. Dissolution Study. The comparative *in vitro* dissolution profile of pure ATV, PM3 (1:4), or optimized ATV-PECE-SD3 (1:4) formulations in phosphate buffer (0.05 M, pH 6.8) was performed using the USP type II paddle dissolution test apparatus (Model: TDT-08LX, Electrolab India Pvt. Ltd., Mumbai, India). The dissolution studies were carried out according to the procedure reported earlier in the literature.[51] Briefly, the samples of pure ATV (~40 mg), PM3 (1:4) (~40 mg of ATV), or optimized ATV-PECE-SD3 (1:4) formulations (equivalent to ~40 mg of ATV) were accurately weighed and dispersed into 900 mL of dissolution media. The dispersed samples were magnetically stirred at a speed of 100 RPM. The temperature of the dissolution medium was set at 37 ± 0.5 °C for 2 h. At the scheduled time interval, the small aliquot of the sample was removed and replenished with fresh media to maintain the sink conditions. The removed samples were diluted suitably and subjected to spectrophotometer analysis (Model: V-630, Jasco International Co., Ltd., Tokyo, Japan) for ATV absorbance at a maximum wavelength of ~240 nm against the blank solution. The absorbance values of pure ATV, PM3, or ATV-PECE-SD3 (1:4) formulations were calculated, and the percentage cumulative of ATV release was reported.

4.13. DE Study. The DE was used to analyze the dissolution profiles of drugs and formulations.[52] The dissolution efficiency of pure ATV and optimized ATV-PECE-SD3 (1:4) formulations in phosphate buffer was calculated using eq 1.

$$\text{DE} = 1 + \frac{\int_{t1}^{t2} y \cdot \mathrm{d}t}{y100 \times (t_2 - t_1)} \times 100 \tag{1}$$

In the above equation, the term y shows the percentage of ATV dissolved in phosphate buffer, whereas the DE shows the AUC of the dissolution curve between the t_1 and t_2 time points. It is expressed in the percentage of maximum dissolution of $y100$ over the same period. The numerator part of the DE was estimated by employing the earlier described equation.

The AUC was calculated using the below-described equation.

$$\text{AUC} = \sum_{i=1}^{i=n} - \frac{(t_1 - t_i - 1)(Y_i - 1 + Y_i)}{2} \tag{2}$$

According to this equation, the t_i shows the ith time points, and Y_i shows the percentage of ATV dissolved at time t_i. The DDSolver program was used further to estimate the DE of pure ATV and optimized ATV-PECE-SD3 (1:4) formulations.

4.14. Fasted vs Fed State Dissolution Comparison Studies. The effect of the fasted vs fed state on the dissolution performance of pure ATV or optimized ATV-PECE-SD3 (1:4) formulations was analyzed using the USP type II paddle dissolution test apparatus (Model: TDT-08LX, Electrolab India Pvt. Ltd., Mumbai, India). The dissolution media, *i.e.*, fasted state simulated intestinal fluid (FaSSIF) and fed state simulated intestinal fluid (FeSSIF), were prepared using the procedure reported earlier in the literature.[42] Briefly, the

samples of pure ATV (~40 mg) or optimized ATV-PECE-SD3 (1:4) formulations (~40 mg of ATV) were accurately weighed and dispersed in FaSSIF (~500 mL) or FeSSIF (~1000 mL) dissolution media. The samples were stirred at a speed of 50 RPM. The media temperature was set at $37 \pm 0.5\ ^{\circ}C$ for 2 h. At the scheduled time interval, the samples were removed and replaced with fresh dissolution media. The removed samples were diluted suitably and subjected to spectrophotometer analysis (Model: V-630, Jasco International Co., Ltd., Tokyo, Japan) at a maximum wavelength of ~239 nm for FaSSIF and ~284 nm for FeSSIF against the blank. The recorded absorbance values were calculated, and the cumulative percentage of ATV release was reported.

4.15. Permeation Studies. The comparative permeation performance of pure ATV, PM3 (1:4), or optimized ATV-PECE-SD3 (1:4) formulations across the everted rat intestinal membrane was analyzed using a specially designed everted rat intestine apparatus reported earlier in the literature.[53,54] The source of animals (rat intestine) was used from Central Preclinical Research Facility, Datta Meghe Institute of Higher Education and Research (DMIHER), (DU), Wardha, Maharashtra, India. The preparation of permeation media and everted rat intestine membrane was done using the procedure described earlier.[10] Briefly, the prepared everted rat intestine membrane was washed and fixed between the two tapered ends of the apparatus. The apparatus was filled with freshly prepared Kreb's solution and submerged into a 250 mL beaker containing test solutions of pure ATV (~100 μg/mL), PM3 (1:4) (~100 μg/mL), or optimized ATV-PECE-SD3 (1:4) formulations (~100 μg/mL of ATV). The permeation medium was stirred at 25 RPM, and its temperature was maintained at $37 \pm 0.5\ ^{\circ}C$ for 2 h. The media was also aerated using a 95% O_2 and 5% CO_2 mixture. At the scheduled interval, a small aliquot of the sample was removed, filtered, diluted, and subjected to spectrophotometer analysis (Model: V-630, Jasco International Co., Ltd., Tokyo, Japan) for ATV absorbance at a maximum wavelength of ~241 nm against the blank solution. The comparative absorbance values of pure ATV, PM, or formulations were calculated, and the cumulative % of ATV permeation was reported.

4.16. Stability Studies. The effect of controlled temperature ($25 \pm 5\ ^{\circ}C$) and relative humidity ($60 \pm 5\%$ RH) on the *in vitro* dissolution and *ex vivo* permeation performance of ATV from optimized ATV-PECE-SD3 (1:4) formulations was carried out using the procedure reported earlier.[54] Briefly, screw-capped high-density polyethylene glass bottles loaded with optimized ATV-PECE-SD3 (1:4) formulations were transferred and stored in a stability chamber (model: TS00002009, Mumbai, Maharashtra, India) for 6 months. After 6 months, the formulations were analyzed for dissolution and permeation studies.

4.17. Statistical Analysis. Dunnett's or Bonferroni's test was employed for statistical analysis to compare the differences between the test samples. The results are presented as mean $\pm$ standard deviation. The P-value of less than 0.05 was considered statistically significant.

■ AUTHOR INFORMATION

Corresponding Author

    Darshan R. Telange — *Datta Meghe College of Pharmacy, Datta Meghe Institute of Higher Education and Research (Deemed to be University), Wardha 442002 Maharashtra,*

India; ● orcid.org/0000-0003-3016-8237; Phone: 0712-287701; Email: darshan.pharmacy@dmiher.edu.in

Authors

    Neha M. Bhaktani — *Smt. Kishoritai Bhoyar College of Pharmacy, Nagpur 441002 Maharashtra, India*

    Atul T. Hemke — *Smt. Kishoritai Bhoyar College of Pharmacy, Nagpur 441002 Maharashtra, India*

    Anil M. Pethe — *Datta Meghe College of Pharmacy, Datta Meghe Institute of Higher Education and Research (Deemed to be University), Wardha 442002 Maharashtra, India*

    Surendra S. Agrawal — *Datta Meghe College of Pharmacy, Datta Meghe Institute of Higher Education and Research (Deemed to be University), Wardha 442002 Maharashtra, India*

    Nilesh R. Rarokar — *Rashtrasant Tukadoji Maharaj Nagpur University, Department of Pharmaceutical Sciences, Mahatma Jyotiba Fuley Shaik Shanik Parisar, University Campus, Nagpur 440033 Maharashtra, India;* ● orcid.org/0000-0003-3401-7997

    Shirish P. Jain — *Rajarshi Shahu College of Pharmacy, Buldana 443001 Maharashtra, India*

Complete contact information is available at:
https://pubs.acs.org/10.1021/acsomega.3c02280

Notes

The authors declare no competing financial interest.

■ LIST OF ABBREVIATIONS

ATV:atorvastatin; PECE:pentaerythritol-eudragitRS100 co-processed excipients; SD:solid dispersions; ERS100:eudragitRS100; ATV-PECE-SD:atorvastatin-pentaerythritol-eudragitRS100 co-processed excipient-solid dispersions; SEM:scanning electron microscopy; DSC:differential scanning calorimetry; PXRD:powder x-ray diffractometry; FT-IR:Fourier transform infrared spectroscopy; FaSSIF:fasted state simulated intestinal fluid; FeSSIF:fed state simulated intestinal fluid; DF:dissolution efficiency; PM:physical mixture; PCCS:photon cross-correlation spectroscopy; DLS:dynamic light scattering

■ REFERENCES

(1) Rodde, M. S.; Divase, G. T.; Devkar, T. B.; Tekade, A. R. Solubility and Bioavailability Enhancement of Poorly Aqueous Soluble Atorvastatin: In Vitro, Ex Vivo, and in Vivo Studies. *Biomed. Res. Int.* **2014**, *2014*, 1−11.

(2) Lau, Y. Y.; Okochi, H.; Huang, Y.; Benet, L. Z. Pharmacokinetics of Atorvastatin and Its Hydroxy Metabolites in Rats and the Effects of Concomitant Rifampicin Single Doses: Relevance of First-Pass Effect from Hepatic Uptake Transporters, and Intestinal and Hepatic Metabolism. *Drug Metab. Dispos.* **2006**, *34*, 1175−1181.

(3) Shete, G.; Puri, V.; Kumar, L.; Bansal, A. K. Solid State Characterization of Commercial Crystalline and Amorphous Atorvastatin Calcium Samples. *AAPS PharmSciTech* **2010**, *11*, 598−609.

(4) Pusapati, R.; Rapeti, S.; Kumar, Mvrk.; Murthy, T. Development of Co-Processed Excipients in the Design and Evaluation of

Atorvastatin Calcium Tablets by Direct Compression Method. *Int. J. Pharm. Invest.* **2014**, *4*, 102.

(5) Jahangiri, A.; Barzegar-Jalali, M.; Javadzadeh, Y.; Hamishehkar, H.; Adibkia, K. Physicochemical Characterization of Atorvastatin Calcium/Ezetimibe Amorphous Nano-Solid Dispersions Prepared by Electrospraying Method. *Artif. Cells, Nanomed., Biotechnol.* **2017**, *45*, 1138−1145.

(6) Shaker, M. A. Dissolution and Bioavailability Enhancement of Atorvastatin: Gelucire Semi-Solid Binary System. *J. Drug Delivery Sci. Technol.* **2018**, *43*, 178−184.

(7) Al-Kazemi, R.; Al-Basarah, Y.; Nada, A. Dissolution Enhancement of Atorvastatin Calcium by Cocrystallization. *Adv. Pharm. Bull.* **2019**, *9*, 559−570.

(8) Sharma, M.; Mehta, I. Surface Stabilized Atorvastatin Nanocrystals With Improved Bioavailability, Safety and Antihyperlipidemic Potential. *Sci. Rep.* **2019**, *9*, No. 16105.

(9) Faraji, E.; Mohammadi, M.; Mahboobian, M. M. Development of the Binary and Ternary Atorvastatin Solid Dispersions: In Vitro and in Vivo Investigations. *Biomed Res. Int.* **2021**, *2021*, No. 6644630.

(10) Dhore, P. W.; Dave, V. S.; Saoji, S. D.; Bobde, Y. S.; Mack, C.; Raut, N. A. Enhancement of the Aqueous Solubility and Permeability of a Poorly Water Soluble Drug Ritonavir via Lyophilized Milk-Based Solid Dispersions. *Pharm. Dev. Technol.* **2017**, *22*, 90−102.

(11) Manaspon, C.; Viravaidya-Pasuwat, K.; Pimpha, N. Preparation of Folate-Conjugated Pluronic F127/Chitosan Core-Shell Nanoparticles Encapsulating Doxorubicin for Breast Cancer Treatment. *J. Nanomater.* **2012**, *2012*, 1−12.

(12) Apeji, Y. E.; Oyi, A. R.; Isah, A. B.; Allagh, T. S.; Modi, S. R.; Bansal, A. K. Development and Optimization of a Starch-Based Co-Processed Excipient for Direct Compression Using Mixture Design. *AAPS PharmSciTech* **2018**, *19*, 866−880.

(13) Saha, S.; Shahiwala, A. F. Multifunctional Coprocessed Excipients for Improved Tabletting Performance. *Expert Opin. Drug Delivery* **2009**, *6*, 197−208.

(14) Karavas, E.; Georgarakis, E.; Sigalas, M. P.; Avgoustakis, K.; Bikiaris, D. Investigation of the Release Mechanism of a Sparingly Water-Soluble Drug from Solid Dispersions in Hydrophilic Carriers Based on Physical State of Drug, Particle Size Distribution and Drug-Polymer Interactions. *Eur. J. Pharm. Biopharm.* **2007**, *66*, 334−347.

(15) Bikiaris, D.; Papageorgiou, G. Z.; Stergiou, A.; Pavlidou, E.; Karavas, E.; Kanaze, F.; Georgarakis, M. Physicochemical Studies on Solid Dispersions of Poorly Water-Soluble Drugs: Evaluation of Capabilities and Limitations of Thermal Analysis Techniques. *Thermochim. Acta* **2005**, *439*, 58−67.

(16) Al-Hamidi, H.; Edwards, A. A.; Mohammad, M. A.; Nokhodchi, A. To Enhance Dissolution Rate of Poorly Water-Soluble Drugs: Glucosamine Hydrochloride as a Potential Carrier in Solid Dispersion Formulations. *Colloids Surf., B* **2010**, *76*, 170−178.

(17) Vasconcelos, T.; Sarmento, B.; Costa, P. Solid Dispersions as Strategy to Improve Oral Bioavailability of Poor Water Soluble Drugs. *Drug Discovery Today* **2007**, *12*, 1068−1075.

(18) Surini, S.; Evangelista, C. N.; Iswandana, R. Development of Glimepiride Solid Dispersion Using the Coprocessed Excipients of Polyvinylpyrrolidone, Maltodextrin, and Polyethylene Glycol. *J. Young Pharm.* **2018**, *10*, s45−s50.

(19) Dave, V.; Telange, D.; Denge, R.; Patil, A.; Umekar, M.; Gupta, S. V. Pentaerythritol as an Excipient/Solid-Dispersion Carrier for Improved Solubility and Permeability of Ursodeoxycholic Acid. *J. Excipients Food Chem.* **2018**, *9*, 80−95.

(20) Adibkia, K.; Javadzadeh, Y.; Dastmalchi, S.; Mohammadi, G.; Niri, F. K.; Alaei-Beirami, M. Naproxen-EudragitRS100 Nanoparticles: Preparation and Physicochemical Characterization. *Colloids Surf., B* **2011**, *83*, 155−159.

(21) Chiou, W. L.; Reigelman, S. Preparation and Dissolution Characteristics of Several Fast-Release Solid Dispersion of Griseofulvin. *J. Pharm. Sci.* **1969**, *58*, 1505−1510.

(22) Barzegar-Jalali, M.; Alaei-Beirami, M.; Javadzadeh, Y.; Mohammadi, G.; Hamidi, A.; Andalib, S.; Adibkia, K. Comparison of Physicochemical Characteristics and Drug Release of Diclofenac

Sodium-EudragitRS100 Nanoparticles and Solid Dispersions. *Powder Technol.* **2012**, *219*, 211−216.

(23) Kim, J. S.; Kim, M. S.; Park, H. J.; Jin, S. J.; Lee, S.; Hwang, S. J. Physicochemical Properties and Oral Bioavailability of Amorphous Atorvastatin Hemi-Calcium Using Spray-Drying and SAS Process. *Int. J. Pharm.* **2008**, *359*, 211−219.

(24) Choudhary, A.; Rana, A. C.; Aggarwal, G.; Kumar, V.; Zakir, F. Development and Characterization of an Atorvastatin Solid Dispersion Formulation Using Skimmed Milk for Improved Oral Bioavailability. *Acta Pharm. Sin. B* **2012**, *2*, 421−428.

(25) Manjunath, K.; Ready, J. S.; Venkateswarlu, V. Solid Lipid Nanoparticles as Drug Delivery Systems. *Methods Find. Exp. Clin. Pharmacol.* **2005**, *27*, 127−144.

(26) Rarokar, N. R.; Saoji, S. D.; Raut, N. A.; Taksande, J. B.; Khedekar, P. B.; Dave, V. S. Nanostructured Cubosomes in a Thermoresponsive Depot System: An Alternative Approach for the Controlled Delivery of Docetaxel. *AAPS PharmSciTech* **2016**, *17*, 436−445.

(27) Mazumder, A.; Dwivedi, A.; Du Preez, J. L.; Du Plessis, J. In Vitro Wound Healing and Cytotoxic Effects of Sinigrin-Phytosome Complex. *Int. J. Pharm.* **2016**, *498*, 283−293.

(28) Iqbal, R.; Qureshi, O. S.; Yousaf, A. M.; Raza, S. A.; Sarwar, H. S.; Shahnaz, G.; Saleem, U.; Sohail, M. F. Enhanced Solubility and Biopharmaceutical Performance of Atorvastatin and Metformin via Electrospun Polyvinylpyrrolidone-Hyaluronic Acid Composite Nanoparticles. *Eur. J. Pharm. Sci.* **2021**, *161*, No. 105817.

(29) Kamran, M.; Khan, M. A.; Shafique, M.; Rehman, M. ur.; Ahmed, W.; Abdullah; Ahmad, S. Development and Characterization of Binary Solid Lipid Nano Suspension of Atorvastatin: In-Vitro Drug Release and In-Vivo Pharmacokinetic Studies. *Nanosci. Nanotechnol. Lett.* **2019**, *11*, 1522−1530.

(30) Ramamoorthy, P.; Krishnamurthy, N. Vibration Spectrum of Pentaerythritol. *Spectrochim. Acta, Part A* **1997**, *53*, 655−663.

(31) Chaheen, M.; Sanchez-Ballester, N. M.; Bataille, B.; Yassine, A.; Belamie, E.; Sharkawi, T. Development of Coprocessed Chitin-Calcium Carbonate as Multifunctional Tablet Excipient for Direct Compression. *J. Pharm. Sci.* **2018**, *107*, 2152−2159.

(32) Balcerowiak, W. Comments On Pentaerythritol DSC. *J. Therm. Anal.* **1996**, *46*, 1881−1883.

(33) Alshaya, H. A.; Alfahad, A. J.; Alsulaihem, F. M.; Aodah, A. H.; Alshehri, A. A.; Almughem, F. A.; Alfassam, H. A.; Aldossary, A. M.; Halwani, A. A.; Bukhary, H. A.; Badr, M. Y.; Massadeh, S.; Alaamery, M.; Tawfik, E. A. Fast-Dissolving Nifedipine and Atorvastatin Calcium Electrospun Nanofibers as a Potential Buccal Delivery System. *Pharmaceutics* **2022**, *14*, No. 358.

(34) Payab, S.; Davaran, S.; Tanhaei, A.; Fayyazi, B.; Jahangiri, A.; Farzaneh, A.; Adibkia, K. Triamcinolone Acetonide-EudragitRS100 Nanofibers and Nanobeads: Morphological and Physicochemical Characterization. *Artif. Cells, Nanomed., Biotechnol.* **2016**, *44*, 362−369.

(35) Goldberg, H.; Gibaldit, M.; Joseph, K.; Mayorshon, M. Increasing Dissolution Rates and Gastrointestinal Absorption of Drugs Via Solid Solutions and Eutectic Mixtures IV. *J. Pharm. Innov.* **1995**, *314*, 307−314.

(36) Goldberg, H.; Gibaldi, M. Increasing Dissolution Rates and Gastrointestinal Absorption of Drugs via Solid Solutions and Eutectic Mixtures III Experimental Evaluation of Griseofulvin-Succinic Acid Solid Solution. *J. Pharm. Sci.* **1966**, *55*, 487−492.

(37) Leuner, C.; Dressman, J. Improving Drug Solubility for Oral Delivery Using Solid Dispersions. *Eur. J. Pharm. Biopharm.* **2000**, *50*, 47−60.

(38) Pignatello Davide Amico Santina C, R.; Amico, D.; Chiechio, S.; Spadaro, C.; Puglisi, G.; Giunchedi, P. Preparation and Analgesic Activity of Eudragit RS100 Microparticles Containing Diflunisal. *Drug Delivery* **2001**, *8*, 35−45.

(39) Shivakumar, H.; Desai, B.; Deshmukh, G. Design and Optimization of Diclofenac Sodium Controlled Release Solid Dispersions by Response Surface Methodology. *Indian J. Pharm. Sci.* **2008**, *70*, 22−30.

(40) Konno, H.; Handa, T.; Alonzo, D. E.; Taylor, L. S. Effect of Polymer Type on the Dissolution Profile of Amorphous Solid Dispersions Containing Felodipine. *Eur. J. Pharm. Biopharm.* **2008**, *70*, 493−499.

(41) Hussain, M. D.; Saxena, V.; Brausch, J. F.; Talukder, R. M. Ibuprofen-Phospholipid Solid Dispersions: Improved Dissolution and Gastric Tolerance. *Int. J. Pharm.* **2012**, *422*, 290−294.

(42) Klein, S. The Use of Biorelevant Dissolution Media to Forecast the in Vivo Performance of a Drug. *AAPS J.* **2010**, *12*, 397−406.

(43) Raman, S.; Polli, J. E. Prediction of Positive Food Effect: Bioavailability Enhancement of BCS Class II Drugs. *Int. J. Pharm.* **2016**, *506*, 110−115.

(44) Belgamwar, V. S.; Dharashivkar, S. S.; Dave, V. S.; Mack, C.; Rode, A. A.; Saoji, S. D. The Study of the Influence of Formulation and Process Variables on the Functional Attributes of Simvastatin− Phospholipid Complex. *J. Pharm. Innov.* **2016**, *11*, 264−278.

(45) Telange, D. R.; Jain, S. P.; Pethe, A. M.; Kharkar, P. S. Egg White Protein Carrier-Assisted Development of Solid Dispersion for Improved Aqueous Solubility and Permeability of Poorly Water Soluble Hydrochlorothiazide. *AAPS PharmSciTech* **2021**, *22*, No. 94.

(46) Telange, D. R.; Patil, A. T.; Pethe, A. M.; Fegade, H.; Anand, S.; Dave, V. S. Formulation and Characterization of an Apigenin-Phospholipid Phytosome (APLC) for Improved Solubility, in Vivo Bioavailability, and Antioxidant Potential. *Eur. J. Pharm. Sci.* **2017**, *108*, 36−49.

(47) Telange, D. R.; Patil, A. T.; Pethe, A. M.; Tatode, A. A.; Anand, S.; Dave, V. S. Kaempferol-Phospholipid Complex: Formulation, and Evaluation of Improved Solubility, in Vivo Bioavailability, and Antioxidant Potential of Kaempferol. *J. Excipients Food Chem.* **2016**, *7*, 89−116.

(48) Nirgulkar, S. B.; Bali, N. R.; Pethe, A. M.; Telange, D. R.; Umekar, M. J.; Patil, A. T. Enhanced Transdermal Permeation and Anti-Inflammatory Potential of Phospholipids Complex-Loaded Matrix Film of Umbelliferone: Formulation Development, Physico-Chemical and Functional Characterization. *Eur. J. Pharm. Sci.* **2019**, *131*, 23−38.

(49) Telange, D. R.; Sohail, N. K.; Hemke, A. T.; Kharkar, P. S.; Pethe, A. M. Phospholipid Complex-Loaded Self-Assembled Phytosomal Soft Nanoparticles: Evidence of Enhanced Solubility, Dissolution Rate, Ex Vivo Permeability, Oral Bioavailability, and Antioxidant Potential of Mangiferin. *Drug Delivery Transl. Res.* **2021**, *11*, 1056−1083.

(50) Telange, D. R.; Jain, S. P.; Pethe, A. M.; Kharkar, P. S.; Rarokar, N. R. Use of Combined Nanocarrier System Based on Chitosan Nanoparticles and Phospholipids Complex for Improved Delivery of Ferulic Acid. *Int. J. Biol. Macromol.* **2021**, *171*, 288−307.

(51) Dhore, P. W.; Dave, V. S.; Saoji, S. D.; Gupta, D.; Raut, N. A. Influence of Carrier (Polymer) Type and Drug-Carrier Ratio in the Development of Amorphous Dispersions for Solubility and Permeability Enhancement of Ritonavir. *J. Excipients Food Chem.* **2017**, *8*, 75−92.

(52) Anderson, N. H.; Bauer, M.; Boussac, N.; Khan-Malek, R.; Munden, P.; Sardaro, M. An Evaluation of Fit Factors and Dissolution Efficiency for the Comparison of in Vitro Dissolution Profiles. *J. Pharm. Biomed. Anal.* **1998**, *17*, 811−822.

(53) Dixit, P.; Jain, D. K.; Dumbwani, J. Standardization of an Ex Vivo Method for Determination of Intestinal Permeability of Drugs Using Everted Rat Intestine Apparatus. *J. Pharmacol. Toxicol. Methods* **2012**, *65*, 13−17.

(54) Telange, D. R.; Bhagat, S. B.; Patil, A. T.; Umekar, M. J.; Pethe, A. M.; Raut, N. A.; Dave, V. S. Glucosamine HCL-Based Solid Dispersions to Enhance the Biopharmaceutical Properties of Acyclovir. *J. Excipients Food Chem.* **2019**, *10*, 65−81.